Nanoscale

PAPER

View Article Online
View Journal | View Issue

Cite this: *Nanoscale*, 2015, **7**, 7437

Does a nitrogen matter? Synthesis and photoinduced electron transfer of perylenediimide donors covalently linked to $C_{59}N$ and C_{60} acceptors†

Luis Martín-Gomis,[a] Georgios Rotas,[b] Kei Ohkubo,[c] Fernando Fernández-Lázaro,[a] Shunichi Fukuzumi,*[c,d] Nikos Tagmatarchis*[b] and Ángela Sastre-Santos*[a]

Received 15th January 2015,
Accepted 12th March 2015

DOI: 10.1039/c5nr00308c

www.rsc.org/nanoscale

The first perylenediimide (PDI) covalently linked to an azafullerene ($C_{59}N$) is described. PDI-$C_{59}N$ and PDI-C_{60} dyads where PDI acts as an electron-donor moiety have been synthesized by connection of the balls to the PDI 1-bay position. Photoexcitation of the PDI unit in both systems results in formation of the charge-separated state by photoinduced electron transfer from the singlet excited state of the PDI moiety to the $C_{59}N$ or to the C_{60} moiety. The charge-separated state has a lifetime of 400 ps in the case of PDI-$C_{59}N$ and 120 ps for the PDI-C_{60} dyad in benzonitrile at 298 K. This result has significant implications for the design of organic solar cells based on covalent donor–acceptor systems using $C_{59}N$ as an electron acceptor, indicating that longer-lived charge-separated states can be attained using $C_{59}N$ systems instead of C_{60} systems.

Introduction

The seeking for efficient molecular systems, based on the covalent combination of suitable and versatile building blocks, capable to mimic the photoinduced electron transfer that naturally occurs in photosynthesis, has been a constant in material science.[1] In a simplistic definition, a molecular system which combines an electron-acceptor moiety with an electron-donor counterpart, able to be excited by the action of light, can be considered as a potential photosynthetic system, and therefore useful for photovoltaic applications. [60]Fullerene, due to its extraordinary electron-acceptor character and its fascinating chemical versatility, has been one of the most utilized electron-acceptor building blocks[2] for that purpose and, thus, several efficient artificial photosynthetic [60]fullerene-based systems have been described, using different chromophores as photoexcitable electron-donor counterparts.[3] Performances of these donor–acceptor materials can be improved by selecting an appropriate electron-donor counterpart, but also by replacing one or more carbon atoms of the fullerene cage by heteroatoms, affording the so-called heterofullerenes.[4] The substitution of a tetravalent carbon atom of the three dimensional network by a trivalent nitrogen atom is one of the most interesting alterations. This simple modification leads to azafullerene $C_{59}N$, a fullerene-based building block with an improved electron-acceptor character, when it is compared to that of pristine C_{60} fullerene.[5] A number of different azafullerene-based donor–acceptor covalent compounds have been previously described, showing interesting photophysical properties that make them ideal candidates to be incorporated in organic photovoltaic devices. Hirsch *et al.* described the synthesis of an azafullerene-ferrocene dyad that shows strong electronic coupling between the ferrocene and azafullerene moieties in the ground state.[6] Additional $C_{59}N$-based dyads carrying photoactive units such as porphyrin[7] and pyrene[8] were also prepared. More recently, azafullerene–electron-donor dyads, using phthalocyanine[9] and corrole[10] units, have been reported to undergo photoinduced electron transfer upon selective irradiation of the electron-donor moiety.

On the other hand, perylenediimides (PDI) comprise an outstanding family of perylene derivatives that, due to an extreme synthetic versatility and an easily tunable electronic character, have become one of the most promising classes of molecular materials in organic photovoltaic devices.[11] In this context, we can find only a few examples where PDI derivatives

[a]*Área de Química Orgánica Instituto de Bioingeniería, Universidad Miguel Hernández, Elche, Spain. E-mail: asastre@umh.es; Fax: +34 966658408; Tel: +34 966658351*
[b]*Theoretical and Physical Chemistry Institute, National Hellenic Research Foundation, 48 Vassileos Constantinou Avenue, Athens 116 35, Greece. E-mail: tagmatar@eie.gr*
[c]*Department of Material and Life Science, Graduate School of Engineering, Osaka University, ALCA, Japan Science and Technology Agency (JST), Suita, Osaka 565-0871, Japan. E-mail: fukuzumi@chem.eng.osaka-u.ac.jp*
[d]*Department of Bioinspired Science, Ewha Womans University, Seoul, 120-750, Korea*

† Electronic supplementary information (ESI) available: Characterization spectra of the new compounds. See DOI: 10.1039/c5nr00308c

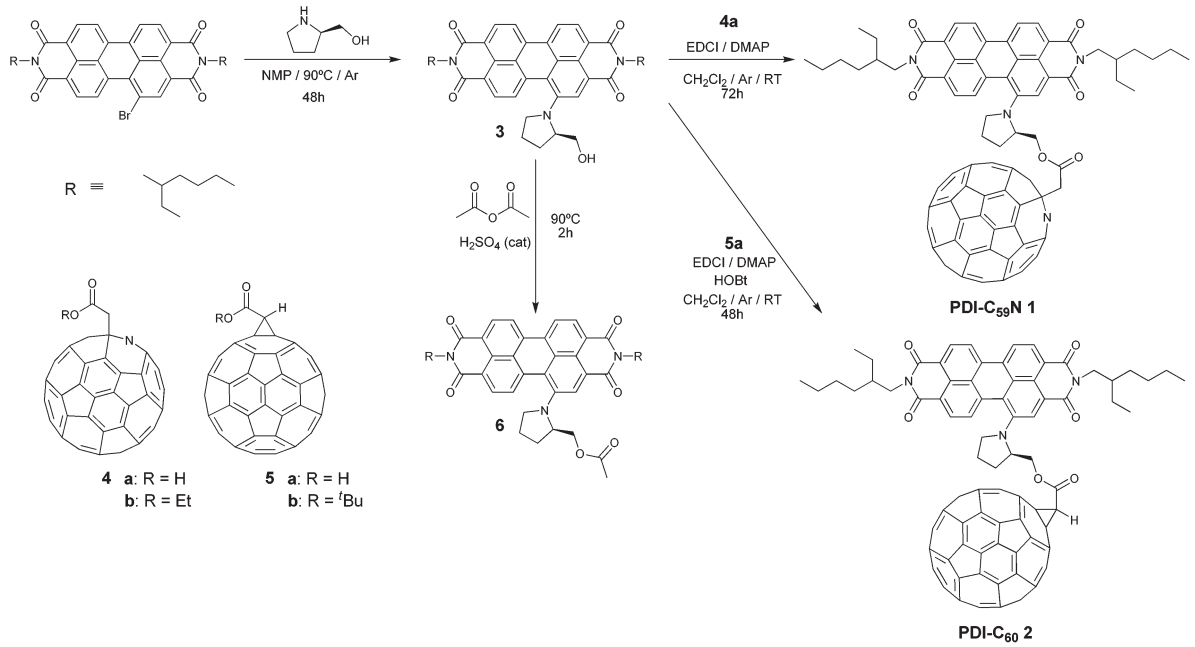

Scheme 1 Synthetic routes for preparing PDI-$C_{59}N$ **1** and PDI-C_{60} **2** dyads as well as PDI-based reference material **6**.

have been successfully employed as an electron-donor moiety in fullerene-based systems, eventually undergoing photoinduced electron and/or energy transfer.[12]

Here we present the synthesis, characterization and photophysical properties of a new photoexcitable molecular system, consisting of an electron-donor PDI moiety, carrying a pyrrolidinyl substituent in the 1-bay position, which also acts as a linker to the $C_{59}N$ counterpart (Scheme 1). The obtained donor–acceptor PDI-$C_{59}N$ dyad **1**, upon selective excitation of the PDI subunit in benzonitrile, shows efficient intramolecular photoinduced electron transfer, generating a 400 ps-lived charge-separated state (CSS). Together with two covalently linked porphyrin-$C_{59}N$ dyads,[7] this is the longest CSS lifetime value obtained so far for a $C_{59}N$-based donor–acceptor dyad in a polar solvent. Moreover, in order to study the effect of the nitrogen atom on the photophysics, the analogous PDI-C_{60} dyad **2** (Scheme 1) was synthesized, as reference material, obtaining a 3-times shorter CSS lifetime than for the PDI-$C_{59}N$ dyad **1**, thus, highlighting the role of nitrogen in the photoinduced electron-transfer processes.

Synthesis and characterization

Initially, PDI-$C_{59}N$ and PDI-C_{60} dyads **1** and **2** were synthesized as described in Scheme 1. Firstly, (*R*)-1-(2′-hydroxymethylpyrrolidin-*N*-yl)PDI **3** was obtained upon nucleophilic aromatic substitution on *N*,*N*′-di(2-ethylhexyl)-1-bromoperylene-3,4,9,10-tetracarboxy diimide[13] by (*R*)-2-hydroxymethylpyrrolidine in 51% yield. Then, the esterification reaction of PDI-based **3** with azafullerenylacetic acid **4a**[9] gave rise to PDI-$C_{59}N$ dyad **1** in 8% yield. A similar esterification process, involving 2,2-[60]fullerenylacetic acid **5a**[14] and PDI-based **3** was followed, affording in 43% yield PDI-C_{60} dyad **2**. Furthermore, PDI derivative **6** was also synthesized in 75% yield, through an acylation of **3** with acetic anhydride in acidic media, in order to be used as a reliable reference to evaluate optical, electrochemical and photophysical properties.

All new compounds were fully characterised using standard analytical techniques such as ^1H and ^{13}C NMR, HR-MS, FT-IR, electronic absorption and photoluminescence. Fig. 1 compares

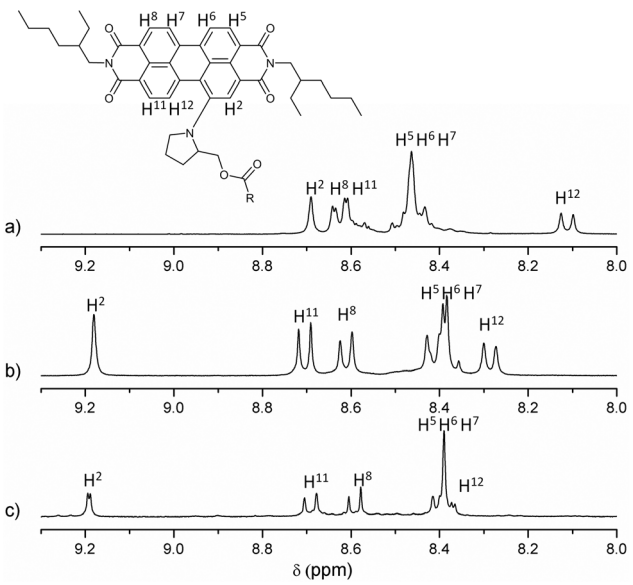

Fig. 1 Partial ^1H NMR (9.30–8.00 ppm) spectra of (a) PDI-based reference material **6**, (b) PDI-C_{60} **2**, and (c) PDI-$C_{59}N$ **1**.

the aromatic region of the ^{1}H NMR spectra for **1**, **2** and **6** in $CDCl_3$ as solvent. Taking as reference the C1 of the PDI core (the substituted one), and comparing the signals of analogous hydrogens in compounds **1**, **2** and **6**, it is worth noting that the chemical displacement of the nearby hydrogens (H^2, H^{11} and H^{12}) is significantly shifted in dyad's spectra, while the contrary trend is observed in the displacement of H^5, H^6, H^7 and H^8. For example, the H^2 signal goes from 8.69 to 9.19 and 9.18 ppm (in **2** and **1** respectively), while H^6 goes from 8.45 to 8.40 ppm. Furthermore, the fullerene influence is slightly larger when $C_{59}N$ is present instead of C_{60}, and it can be recognised in the H^{12} displacement, which changes from 8.11 ppm in **6**, to 8.29 and 8.40 ppm in dyads **2** and **1**, respectively. Fig. 2 shows the aliphatic regions of the spectra, where some differences can also be found due to the presence of the covalently attached fullerene. For example, the signals corresponding to the hydrogens labeled as H^B, H^C and H^E, which appear as broad signals in the spectrum of PDI-based **6**, split into two in the corresponding spectra of PDI-fullerene dyads **1** and **2**. All these differences in the ^{1}H NMR spectra of dyads and reference material can be explained by considering the electron-withdrawing character of the fullerene sphere, which is more intense in the case of $C_{59}N$ as compared with C_{60}, and also assuming a pseudo-fixed molecular conformation in PDI-fullerene dyads caused by an electrostatic interaction between the PDI and the fullerene moiety including a concave–convex interaction[3l,15] that causes a different influence of the sphere on the chemical shift of the pyrrolidine-linker geminal protons. HR MALDI-TOF (negative mode) experiments clearly confirm the structure of PDI-$C_{59}N$ and PDI-C_{60} dyads **1** and **2**, respectively, showing base peaks due to the molecular ions at 1476.463 amu and 1474.302 amu, with isotopical distributions that exactly match the simulated isotope patterns for $C_{106}H_{52}N_4O_6$ and $C_{107}H_{51}N_3O_6$, respectively (see ESI, Fig. S1†).

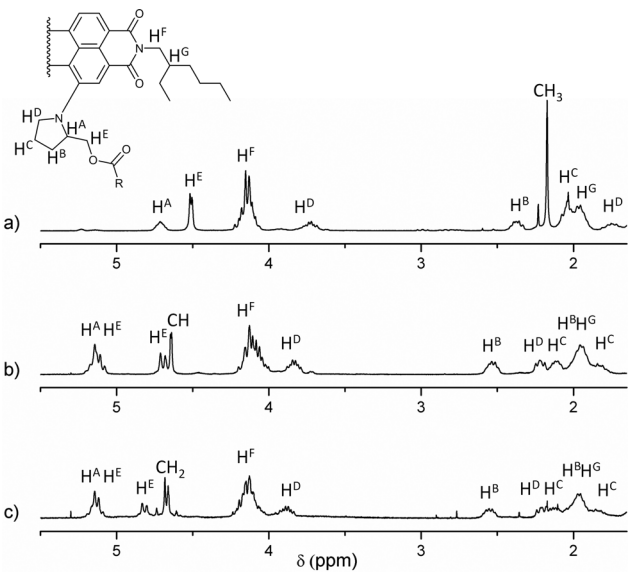

Fig. 2 Partial ^{1}H NMR (5.50–1.60 ppm) spectra in $CDCl_3$ as solvent of (a) PDI-based reference material **6**, (b) PDI-C_{60} **2**, and (c) PDI-$C_{59}N$ **1**.

Photophysical and electrochemical properties

Fig. 3 shows the overlapped UV-vis spectra of dyads **1** (black line) and **2** (blue line) and C_{60} **5a**, $C_{59}N$ **4b** and PDI **6** as reference compounds using benzonitrile as solvent. The absorption spectra of PDI-$C_{59}N$ **1** and PDI-C_{60} **2** dyads are characterised by two sets of absorption maxima around 430 and 638 nm. The band centered at 430 nm can be attributed to transitions 1–0 and 0–0 in the PDI species,[16] while the one centred at 638 nm consists of a broad charge transfer (CT) band that usually appears in bay amino-substituted PDI compounds. The latter band appears as a consequence of an electron transfer between the electron-donor pyrrolidine and the electron-acceptor PDI units,[17] and therefore is very sensitive to changes in the electronic character of the entire molecule. When those spectra are compared to the absorption profile of reference compound PDI **6**, some differences can be found. One of these differences, directly related to the electronic interaction between the electroactive moieties, is a bathochromic displacement of the band centered at 632 nm, which now appears at 638 nm in both PDI-C_{60} and PDI-$C_{59}N$. This fact reveals the electronic influence of the fullerene sphere on the perylene subunit in the ground state, as it has been already pointed out in the comparison of ^{1}H NMR spectra (*cf.* Fig. 1 and 2).

On the other hand, Fig. 4 shows the fluorescence emission spectra of PDI-$C_{59}N$ **1** and PDI-C_{60} **2** dyads, when selectively excited at 429 nm. As can be seen, the fluorescence spectrum of **6** clearly shows three different emission bands, centered at 480, 512 and 691 nm. When the emission spectra of PDI-$C_{59}N$ and PDI-C_{60} dyads **1** and **2** are compared to that of the reference compound, the first and second bands are partially

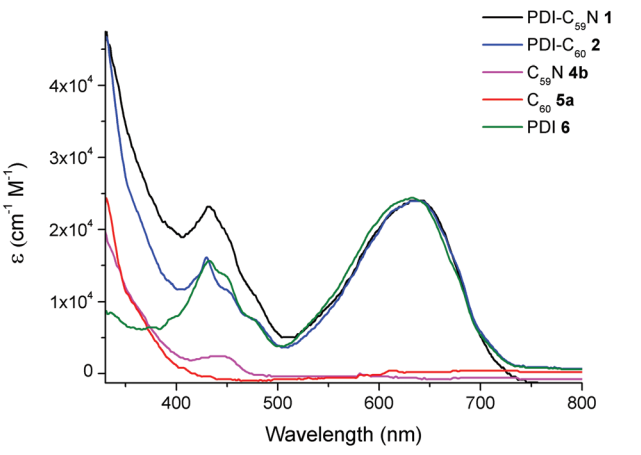

Fig. 3 UV/vis spectra of PDI-$C_{59}N$ **1** and PDI-C_{60} **2**, reference compounds **4b** and **5a** and PDI-based reference **6** registered in benzonitrile as solvent.

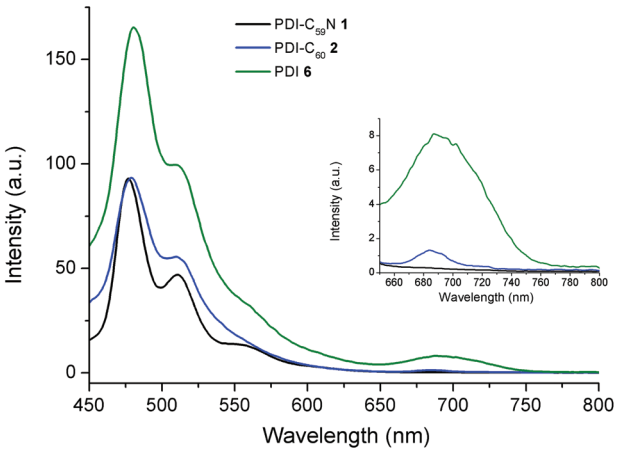

Fig. 4 Fluorescence spectra of PDI-$C_{59}N$ **1** and PDI-C_{60} **2** dyads and PDI-based reference **6**, obtained in benzonitrile (4×10^{-6} M; λ_{exc} = 429 nm). Fluorescence spectra enlargement of **1**, **2** and **6** from 650 to 800 nm.

quenched while the third one is extinguished. The latter is indicative of intra-dyad electronic interactions between the two components of the dyad (*i.e.*, PDI and fullerene) at the excited state. The strong fluorescence quenching of the 691 nm band in both **1** and **2** as compared to **6**, supports electron and/or energy transfer as the decay mechanism of the PDI-centred singlet excited state. This effect is slightly more pronounced in the case of PDI-$C_{59}N$ dyad **1** (see inset Fig. 4).

The electrochemical data of PDI-$C_{59}N$ **1** and PDI-C_{60} **2** dyads, as well as **6**, **4b** and **5b** as reference materials for PDI-$C_{59}N$, and C_{60}, respectively, in benzonitrile using Fc/Fc^+ as an internal standard are listed in Table 1 (see differential pulse voltammograms in ESI, Fig. S13†). The measurements for PDI **6** reveal a one-electron oxidation and two one-electron reduction processes centred at 0.55, −1.15 and −1.35 V respectively, while the measurements for fullerene reference compounds show two one-electron reversible reduction processes at −1.01 and −1.42 V. The voltammograms of dyads **1** and **2** are very similar, in spite of the nitrogen atom in dyad **1**, and can be considered as a combination of the already mentioned electrochemical processes assigned to PDI and fullerene electroactive moieties. A slight influence of the fullerene sphere (either $C_{59}N$ or C_{60}) over the PDI moiety can be recognised, and it is highlighted by a 20–30 mV anodic displacement of the oxidation wave and a 40 mV cathodic displacement of the second reduction process, which is attributed to the PDI counterpart. As contrary to previous results reported by us,[9,10] the similar first reduction values obtained for PDI-C_{60} and PDI-$C_{59}N$ might come from the use of different solvents. Based on the redox data shown in Table 1 and neglecting the Coulombic interactions, the electrochemical band gap for **1** is calculated as 1.59 eV (1.61 eV for **2**).

Femtosecond laser flash photolysis on a deaerated benzonitrile solution of **1** and **2** indicates the formation of a charge-separated state, providing solid evidence for the electron-transfer deactivation mechanism in **1** and **2**, after selective excitation of the perylene moiety. The transient absorption spectrum taken at 1 ps after laser pulse irradiation of the absorption band of the PDI moiety at 490 nm exhibits an absorption maximum at 900 nm, which is assigned to the singlet excited state of $C_{59}N$ of PDI-$C_{59}N$ dyad **1** (Fig. 5a). No indication of the PDI singlet excited state was observed in spite of the selective excitation of PDI, indicating that the rate of energy transfer from the singlet excited state of the PDI moiety to the $C_{59}N$ moiety is too fast to be followed even with the use of femtosecond laser flash photolysis (fwhm = 130 fs). Then, electron transfer from PDI to the singlet-excited state of $C_{59}N$ takes place to form $PDI^{\bullet+}$-$C_{59}N^{\bullet-}$ as the charge-separated state. The transient absorption band decayed with a rate constant of 5.5×10^{10} s^{-1} giving rise to an absorption band at λ_{max} = 1030 nm due to the $C_{59}N^{\bullet-}$ radical anion,[9,10] which indicates the formation of the charge-separated state. From the decay of the absorption band at 1030 nm, a 400 ps lifetime ($k = 2.5 \times 10^9$ s^{-1}) was obtained for the charged-separated state (Fig. 5b), being the first example of a charge-separated state in a donor–acceptor dyad based on PDI and azafullerene.

When benzonitrile was replaced by toluene, the rate constant of charge separation became much larger (3.9×10^{11} s^{-1}), whereas the rate constant of charge recombination became smaller (1.3×10^9 s^{-1}) as shown in Fig. S14 (ESI†). The faster charge separation in toluene than in benzonitrile may result

Table 1 Redox potentials of PDI-$C_{59}N$ **1** and PDI-C_{60} **2** dyads and **6**, **4b** and **5b** as reference materials for PDI, $C_{59}N$, and C_{60}, respectively. The values are *versus* Fc/Fc^+ and extracted from differential pulse voltammograms of PhCN solutions containing Bu_4NPF_6 (0.10 M) as a supporting electrolyte

	E^3_{red} (V)	E^2_{red} (V)	E^1_{red} (V)	E_{ox} (V)
PDI-**6**	−1.35	−1.15		0.55
PDI-C_{60} **2**	−1.39	−1.19	−1.03	0.58
PDI-$C_{59}N$ **1**	−1.38	−1.19	−1.01	0.58
C_{60}-ref **5b**	−1.42		−1.01	
$C_{59}N$-ref **4b**	−1.42		−1.01	

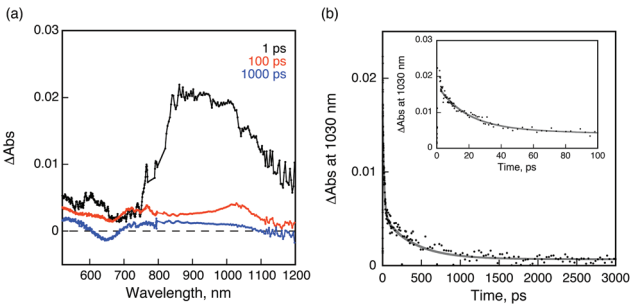

Fig. 5 (a) Transient absorption spectra of $C_{59}N$-PDI (0.5 mM) in deaerated PhCN after femtosecond laser excitation at 510 nm; (b) time profile of the absorbance at 1030 nm. Inset: decay time profile for the short time range. Gray line is drawn by the double exponential curve fitting.

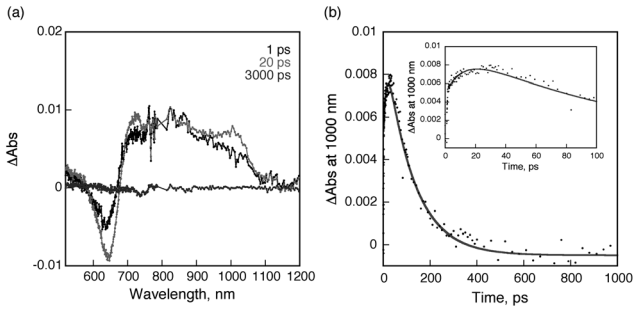

Fig. 6 (a) Transient absorption spectra of C_{60}-PDI (0.5 mM) in deaerated PhCN after femtosecond laser excitation at 510 nm; (b) Time profile of the absorbance at 1000 nm. Inset: rise and decay time profile for the short time range. Gray line is drawn by the double exponential curve fitting.

from the smaller solvent reorganization energy of toluene than that of the more polar benzonitrile in the Marcus normal region, where the charge separation becomes faster with decreasing the solvent reorganisation energy of electron transfer.[1d,18] By the same token, the slower charge recombination in toluene than in benzonitrile results from the smaller solvent reorganisation energy of toluene than that of benzonitrile in the Marcus inverted region, where the charge recombination becomes slower with decreasing the solvent reorganisation energy of electron transfer.[1d,18]

On the other hand, a similar transient absorption spectral change was observed for PDI-C_{60} dyad **2** as shown in Fig. 6a. The transient absorption recorded at 1 ps after femtosecond laser pulse irradiation is assigned to the singlet excited state of C_{60}, indicating that ultrafast energy transfer from the singlet excited state of PDI to the C_{60} moiety also occurs in PDI-C_{60}. Then, electron transfer from PDI to the singlet excited state of C_{60} takes place to form the charge-separated state. The rate constant for electron transfer is determined to be 8.6×10^{10} s^{-1} from the rise of the absorbance at 1000 nm (inset of Fig. 6b). This rate is slightly faster than that of PDI-C_{59}N (*vide supra*). The lifetime of the charge-separated state was determined to be 120 ps from the decay of absorbance at 1000 nm as shown in Fig. 6b. It is worth to mention the much shorter lifetime of the CSS in PDI-C_{60}, less than one third of that in PDI-C_{59}N, pointing to the remarkable influence of the nitrogen atom in C_{59}N, which is not explained only by an increased electron-accepting character as the reduction potentials of **1** and **2** indicate. In both cases, the decay of the charge-separated state by back electron transfer yields the ground state rather than the triplet excited state of PDI as indicated by no triplet transient absorption of **1** and **2** in nanosecond laser flash photolysis measurements (Fig. S14 in ESI†).

Experimental

General information

All chemicals were reagent grade, purchased from commercial sources, and used as received, unless otherwise specified. Column chromatography: SiO_2 (40–63 mm) TLC plates coated with SiO_2 60F254 were visualized by UV light. **2** and **6** crude products were finally purified by a Combiflash Rf chromatography system (Teledyne Technologies, Inc., Thousand Oaks, CA), while **1** crude product was finally purified by preparative HPLC (Japan Analytical Industry Co Ltd, utilising a Buckyprep 20 × 250 column with toluene as eluent at 10 mL min^{-1} flow rate). NMR spectra were measured with a Bruker AC 300. UV/vis spectra were recorded with a Helios Gamma spectrophotometer. Fluorescence spectra were recorded with a PerkinElmer LS 55 Luminescence Spectrometer and IR spectra with a Nicolet Impact 400D spectrophotometer. Mass spectra were obtained from a Bruker Microflex matrix-assisted laser desorption/ionization time of flight (MALDI-TOF).

tert-Butyl (2,2-[60]fullerenyl)acetate **5b** [14] and ethyl (2-azafullerenyl)acetate **4b**, used as C_{60} and C_{59}N reference compounds, respectively, in electrochemistry measurements, were prepared as reported earlier.

Electrochemistry

Differential pulse voltammetry measurements were performed in a conventional three-electrode cell using a μ-AUTOLAB type III potentiostat/galvanostat at 298 K, over PhCN deaerated sample solutions (~0.5 mM), containing 0.10 M tetrabutylammonium hexafluorophosphate ($TBAPF_6$) as supporting electrolyte. A glassy carbon (GC) working electrode, $Ag/AgNO_3$ reference electrode and a platinum wire counter electrode were employed. Ferrocene/ferrocenium was used as an internal standard for all measurements.

Synthesis

Synthesis of *N*,*N*′-di(2-ethylhexyl)-1-[(*R*)-2-(hydroxymethyl)-pyrrolidinyl]perylene-3,4,9,10-tetracarboxy diimide (3). Over a heated solution (90 °C) of (*R*)-2-(hydroxymethyl)pyrrolidine (500 mg, 4.95 mmol), in NMP (10 ml), 100 mg (0.14 mmol) of *N*,*N*′-di(2-ethylhexyl)-1-bromoperylene-3,4,9,10-tetracarboxy diimide suspended in 100 ml of NMP were slowly added under Ar atmosphere. When the addition was completed, the mixture was left at 90 °C continuously stirring for 48 h. The crude product was added over 400 ml of NaOH 1 M, vacuum filtered and washed with distilled water, in order to eliminate the undesirable NMP used as solvent. The crude material was finally purified by column chromatography (SiO_2, Hx→Hx–AcOEt 3 : 1) to obtain 52 mg (51%) of the desired product as a green powder. ^{1}H NMR (300 MHz, 25 °C): 8.46 (1H, s, H-PDI), 8.42–8.35 (2H, m, 3 × H-PDI), 8.18 (1H, d, J = 8.2 Hz, H-PDI), 8.02–7.89 (2H, m, 2 × H-PDI), 7.55–7.47 (1H, m, 2 × H-PDI), 4.51–4.39 (1H, m, C***H***N-pyrrolidine), 4.31 (1H, t, J = 12.7 Hz, C***H***H-OH), 4.21–4.03 (4H, m, 2 × CH_2-*N*-alkyl chain), 3.98 (1H, t, J = 12.7 Hz, CH***H***-OH), 3.57–3.41 (1H, m, CH***H***N-pyrrolidine), 2.30–2.09 (2H, m, CH_2-pyrrolidine), 2.07–1.91 (2H, m, CH***H***-pyrrolidine + CH-alkyl chain), 1.90–1.76 (1H, m, CH-alkyl chain), 1.71–1.59 (2H, m, C***H***HN-pyrrolidine + C***H***H-pyrrolidine) 1.54–1.21 (16H, m, 8 × CH_2-alkyl chain) and 1.06–0.78

(12H, m, 4 × CH_3-alkyl chain) ppm; ^{13}C NMR (75 MHz, $CDCl_3$, 25 °C):164.2, 163.9, 163.3, 163.3, 147.2, 134.8, 134.2, 132.0, 131.5, 129.7, 129.7, 128.3, 128.1, 126.6, 126.2, 124.6, 123.2, 123.0, 122.5, 122.3, 120.6, 120.0, 118.0, 116.2, 62.0, 60.2, 56.2, 44.3, 43.9, 38.1, 38.1, 37.8, 30.9, 30.7, 29.6, 28.8, 28.6, 27.9, 25.2, 24.1, 24.0, 23.1, 14.1, 10.7 and 10.6 ppm; IR-FT (KBr) ν/cm^{-1}: 3467, 2956, 2927, 2858, 1691, 1652, 1586, 1427, 1338, 1242, 807, 748; UV/vis (CH_2Cl_2), λ_{max}/nm ($\log\varepsilon$): 431 (4.16), 637 (4.36); HR-MS (MALDI-TOF, dithranol): m/z = 713.349, [M]$^-$, calcd for $C_{45}H_{51}N_3O_5$: 713.383.

Synthesis of *N*,*N*′-di(2-ethylhexyl)-1-[(*R*)-2-(acetylmethyl)pyrrolidinyl]perylene-3,4,9,10-tetracarboxy diimide (6). 20 mg of **3** (0.03 mmol) were dissolved in 1 ml of acetic anhydride with a catalytic amount of H_2SO_4 (1 drop). The mixture was left, continuously stirred, at 90 °C for 2 h. The crude product was added over 200 ml of NaOH 1 M, extracted with CH_2Cl_2 and, after evaporation of the solvent, purified by Combiflash chromatography (0–5% of AcOEt in CH_2Cl_2). 17 mg of the desired product (75%) were obtained as a green powder. ^{1}H NMR (300 MHz, $CDCl_3$, 25 °C): 8.69 (1H, s, H-PDI), 8.63 (1H, d, J = 8.1 Hz, H-PDI), 8.62 (1H, d, J = 8.0 Hz, H-PDI), 8.52–8.41 (3H, m, 3 × H-PDI), 8.11 (1H, d, J = 8.1 Hz, H-PDI), 4.72 (1H, br s, C***H***N-pyrrolidine), 4.51 (2H, d, J = 3.93 Hz, CH_2-O), 4.23–4.05 (4H, m, 2 × CH_2-*N*-alkyl chain), 3.78–3.68 (1H, m, CH***H***N-pyrrolidine), 2.42–2.32 (2H, m, CH_2-pyrrolidine), 2.17 (3H, s, CH_3-C═O), 2.11–1.88 (4H, m, CH_2-pyrrolidine + 2 × CH-alkyl chain), 1.50–1.24 (16H, m, 8 × CH_2-alkyl chain) and 1.01–0.84 (12H, m, 4 × CH_3-alkyl chain) ppm; ^{13}C NMR (75 MHz, $CDCl_3$, 25 °C): 170.9, 164.3, 164.1, 147.8, 135.9, 135.2, 133.2, 131.3, 129.2, 129.1, 127.6, 127.5, 124.6, 124.0, 123.9, 123.3, 122.9, 122.6, 122.1, 121.0, 119.8, 118.9, 65.3, 57.5, 56.4, 44.5, 38.1, 31.0, 29.1, 28.9, 25.4, 24.3, 23.2, 21.0, 14.3, 10.9, 10.8; IR-FT (KBr) 2956, 2927, 2857, 1744, 1693, 1654, 1587, 1419, 1336, 1240, 808, 748 ν/cm^{-1}; UV/vis (CH_2Cl_2), λ_{max}/nm ($\log\varepsilon$):332 (3.80), 430 (4.17), 624 (4.36); HR-MS (MALDI-TOF, dithranol): m/z = 755.385, [M]$^-$, calcd for $C_{45}H_{51}N_3O_5$: 755.393.

Synthesis of *N*,*N*′-di(2-ethylhexyl)-1-[(*R*)-2-([60]fullereneacetylmethyl)pyrrolidinyl]perylene-3,4,9,10-tetracarboxy diimide (2). Over a suspension of 2,2-([60]fullerenyl)acetic acid[14] (25 mg, 0.034 mmol), **3** (24 mg, 0.034 mmol) and 1-hydroxybenzotriazole (HOBt, 9 mg, 0.067 mmol) in dry dichloromethane (25 mL) at 0 °C under Ar, EDCI (19.5 mg, 0.102 mmol) and DMAP (3 mg, 0.025 mmol) were added. The mixture was left, continuously stirred, at room temperature for 48 h. The reaction was then quenched with HCl 1 M, extracted with CH_2Cl_2 and, after evaporation of solvent, the crude product was purified by Combiflash chromatography (0–5% of AcOEt in $CHCl_3$). 20 mg of the desired product (43%) were obtained as a green powder. ^{1}H NMR (300 MHz, $CDCl_3$, 25 °C): 9.18 (1H, s, H-PDI), 8.70 (1H, d, J = 8.2 Hz, H-PDI), 8.61 (1H, d, J = 8.0 Hz, H-PDI), 8.45–8.35 (3H, m, 3 × H-PDI), 8.29 (1H, d, J = 8.2 Hz, H-PDI), 5.21–5.06 (2H, m, C***H***N-pyrrolidine + C***H***H-O_2C), 4.70 (1H, d, J = 9.3 Hz, CH***H***-O_2C), 4.65 (1H, s, O_2C-C*H*═C_{60}), 4.22–3.99 (4H, m, 2 × CH_2-*N*-alkyl chain), 3.90–3.76 (1H, m, C***H***HN-pyrrolidine), 2.60–2.48 (1H, m, NCH-CH***H***-pyrrolidine), 2.27–1.76 (6H, m, CH***H***N-pyrrolidine + NCH-C***H***H-pyrrolidine + CH_2-pyrrolidine + 2 × CH-alkyl chain), 1.50–1.22 (16H, m, 8 × CH_2-alkyl chain) and 1.01–0.82 (12H, m, 4 × CH_3-alkyl chain) ppm; ^{13}C NMR (75 MHz, $CDCl_3$, 25 °C): 165.8, 164.3, 164.0, 163.9, 148.8, 148.0, 147.0, 145.5, 145.4, 145.2, 145.1, 145.0, 144.9, 144.8, 144.6, 144.5, 144.4, 144.3, 144.2, 144.1, 143.9, 143.7, 143.6, 143.5, 143.4, 143.3, 143.1, 142.9, 142.8, 142.7, 142.5, 142.2, 142.1, 142.0, 141.9, 141.8, 141.2, 141.0, 140.7, 140.2, 140.0, 139.9, 139.2, 136.3, 136.1, 135.6, 135.1, 133.6, 131.5, 131.1, 129.5, 129.0, 127.8, 127.5, 124.9, 124.5, 124.0, 123.7, 123.1, 122.5, 122.1, 121.1, 120.0, 119.4, 70.2, 70.0, 68.9, 57.1, 44.5, 44.4, 44.3, 38.5, 38.2, 38.0, 30.9, 28.9, 28.8, 28.7, 25.4, 24.2, 23.3, 23.2, 14.3 and 10.9; IR-FT (KBr) 2951, 2923, 2854, 1740, 1693, 1655, 1417, 1333, 1242, 1182, 1152, 807, 747, 527 ν/cm^{-1}; UV/vis (CH_2Cl_2), λ_{max}/nm ($\log\varepsilon$): 327 (4.60), 428 (4.18), 628 (4.35); HR-MS (MALDI-TOF, dithranol): m/z = 1473.302, [M]$^-$, calcd for $C_{107}H_{51}N_3O_6$: 1473.378.

Synthesis of *N*,*N*′-di(2-ethylhexyl)-1-[(*R*)-2-(azafullereneacetylmethyl)pyrrolidinyl]perylene-3,4,9,10-tetracarboxy diimide (1). Over a suspension of 2-(azafullerenyl)acetic acid **6** (20 mg, 0.026 mmol), **3** (19 mg, 0.026 mmol) and DMAP (2.5 mg, 0.021 mmol) in dry dichloromethane (20 mL) at 0 °C under N_2, EDCI (15 mg, 0.078 mmol) was added and the mixture was left stirring at r.t. for 72 hours. Then, the solvent was evaporated; the residue was then re-dissolved in *o*-dichlorobenzene (25 mL) and passed through a silica column chromatograph (toluene→toluene–ethyl acetate 9 : 1). The first green fraction was collected and further purified in preparative HPLC (buckyprep, toluene, 10 ml min^{-1}. R.t. = 18.6 min) yielding **1** as green dust (3 mg, 8%). ^{1}H NMR (300 MHz, $CDCl_3$, 25 °C): 9.19 (1H, s, H-PDI), 8.69 (1H, d, J = 8.1 Hz, H-PDI), 8.59 (1H, d, J = 8.0 Hz, H-PDI), 8.44–8.35 (4H, m, 4 × H-PDI), 5.21–5.27 (2H, m, C***H***N-pyrrolidine + C***H***H-O_2C), 4.87–4.77 (1H, m; CH***H***-O_2C), 4.71 (1H, d, J = 16.2 Hz, O_2C-C***H***H-C_{59}N), 4.63 (1H, d, J = 16.2 Hz, O_2C-CH***H***-C_{59}N), 4.24–4.03 (4H, m, 2 × CH_2-*N*-alkyl chain), 3.95–3.83 (1H, m, C***H***HN-pyrrolidine), 2.62–2.48 (1H, m, NCH-CH***H***-pyrrolidine), 2.28–1.76 (6H, m, CH***H***N-pyrrolidine + NCH-C***H***H-pyrrolidine + CH_2-pyrrolidine + 2 × CH-alkyl chain), 1.48–1.22 (16H, m, 8 × CH_2-alkyl chain) and 1.02–0.80 (12H, m, 4 × CH_3-alkyl chain) ppm; ^{13}C NMR (75 MHz, $CDCl_3$, 25 °C): 169.5, 164.5, 164.3, 164.1, 164.0, 154.7, 154.4, 148.5, 147.8, 147.6, 147.5, 147.4, 147.1, 147.0, 146.7, 146.6, 146.5, 146.4, 146.3, 145.9, 145.8, 145.7, 145.1, 145.0, 144.8, 144.6, 144.3, 143.8, 143.6, 143.5, 142.7, 142.1, 141.7, 141.6, 141.1, 140.9, 140.8, 140.6, 139.4, 139.2, 137.0, 136.9, 135.8, 135.2, 134.2, 133.7, 133.6, 131.6, 131.1, 129.4, 129.0, 127.9, 127.6, 124.8, 124.3, 124.1, 123.9, 123.8, 123.6, 123.0, 122.4, 122.0, 121.0, 120.0, 119.2, 78.4, 68.4, 57.4, 57.1, 46.9, 44.5, 44.3, 38.2, 37.9, 30.9, 29.8, 29.1, 28.9, 28.8, 28.7, 25.3, 24.2, 23.3, 23.2, 14.3, 10.9 and 10.8 ppm; IR-FT (KBr) ν/cm^{-1}: 3425, 2953, 2925, 2856, 1747, 1694, 1656, 1588, 1421, 1334, 1242, 1185, 808, 748, 525; UV/vis (CH_2Cl_2), λ_{max}/nm ($\log\varepsilon$): 321 (4.59), 431 (4.27), 632 (4.37); HR-MS (MALDI-TOF, dithranol): m/z = 1476.463, [M]$^-$, calcd for $C_{106}H_{52}N_4O_6$: 1476.389.

Conclusions

We have synthesized for the first time a dyad where a perylenediimide unit is connected to $C_{59}N$. Taking advantage of the electron donor character of the mono pyrrolidinyl PDI derivative synthesised, the PDI-$C_{59}N$ dyad undergoes efficient intramolecular photoinduced electron transfer to afford a 400 ps-lived CS state in PhCN. PDI-C_{60} has also been synthesized, as a reference compound, affording a 3 times shorter CSS lifetime than the PDI-$C_{59}N$ dyad to address the influence of the nitrogen in the photoinduced electron-transfer process. The present results have significant implications for the design of organic solar cells based on covalent donor–acceptor systems using $C_{59}N$ as the acceptor and shows that the longer-lived charge-separated states can be attained using $C_{59}N$ systems instead of C_{60} systems.

Acknowledgements

This work has been supported by the Spanish Ministry of Science and Innovation, Generalitat Valenciana, the European FEDER funds (CTQ2011-26455, PROMETEO 2012/010, ACOMP/2013/024 and ISIC/2012/008), Grants-in-Aid for Scientific Research (no. 26620154 & 26288037) and an Advanced Low Carbon Technology Research and Development (ALCA) and Development of Systems and Technology for Advanced Measurement and Analysis (SENTAN) programs from Japan Science Technology Agency (JST).

Notes and references

1 Recent and interesting reviews on this topic are (*a*) A. C. Benniston and A. Harriman, *Mater. Today*, 2008, **11**, 26–34; (*b*) M. E. El-Khouly, S. Fukuzumi and F. D'Souza, *ChemPhysChem*, 2014, **15**, 30–47; (*c*) S. Berardi, S. Drouet, L. Francas, C. Gimbert-Surinach, M. Guttentag, C. Richmond, T. Stoll and A. Llobet, *Chem. Soc. Rev.*, 2014, **43**, 7501–7519; (*d*) S. Fukuzumi, K. Ohkubo and T. Suenobu, *Acc. Chem. Res.*, 2014, **47**, 1455–1464.

2 (*a*) D. M. Guldi, B. M. Illescas, C. M. Atienza, M. Wielopolskia and N. Martín, *Chem. Soc. Rev.*, 2009, **38**, 1587–1597; (*b*) E. Espildora, J. L. Delgado and N. Martín, *Isr. J. Chem.*, 2014, **54**, 429–439; (*c*) S. Fukuzumi and K. Ohkubo, *J. Mater. Chem.*, 2012, **22**, 4575–4587; (*d*) Y. Kawashima, K. Ohkubo and S. Fukuzumi, *Chem. – Asian J.*, 2015, **10**, 44–54.

3 (*a*) L. Martín-Gomis, K. Ohkubo, F. Fernández-Lázaro, S. Fukuzumi and Á. Sastre-Santos, *Org. Lett.*, 2007, **9**, 3441–3444; (*b*) L. Martín-Gomis, K. Ohkubo, F. Fernández-Lázaro, S. Fukuzumi and Á. Sastre-Santos, *Chem. Commun.*, 2010, **46**, 3944–3946; (*c*) V. Garg, G. Kodis, M. Chachisvilis, M. Hambourger, A. L. Moore, T. A. Moore and D. Gust, *J. Am. Chem. Soc.*, 2011, **133**, 2944–2954; (*d*) T. Fukuda, Y. Kikukawa, S. Takaishi and N. Kobayashi, *Chem. – Asian J.*, 2012, **7**, 751–758; (*e*) E. Krokos, F. Spänig, M. Ruppert, A. Hirsch and D. M. Guldi, *Chem. – Eur. J.*, 2012, **18**, 10427–10435; (*f*) M. E. El-Khouly, C. A. Wijesinghe, V. N. Nesterov, M. E. Zandler, S. Fukuzumi and F. D'Souza, *Chem. – Eur. J.*, 2012, **18**, 13844–13853; (*g*) R. F. Enes, J.-J. Cid, A. Hausmann, O. Trukhina, A. Gouloumis, P. Vázquez, J. A. S. Cavaleiro, A. C. Tomé, D. M. Guldi and T. Torres, *Chem. – Eur. J.*, 2012, **18**, 1727–1736; (*h*) C. B. KC, G. N. Lim, M. E. Zandler and F. D'Souza, *Org. Lett.*, 2013, **15**, 4612–4615; (*i*) W.-J. Shi, M. E. El-Khouly, K. Ohkubo, S. Fukuzumi and D. K. P. Ng, *Chem. – Eur. J.*, 2013, **19**, 11332–11341; (*j*) M. E. El-Khouly, J.-H. Kim, K.-Y. Kay and S. Fukuzumi, *J. Porphyrins Phthalocyanines*, 2013, **17**, 1055–1063; (*k*) R. K. Dubey, M. Niemi, K. Kaunisto, A. Efimov, N. V. Tkachenko and H. Lemmetyinen, *Chem. – Eur. J.*, 2013, **19**, 6791–6806; (*l*) S. Pla, L. Martín-Gomis, K. Ohkubo, S. Fukuzumi, F. Fernández-Lázaro and Á. Sastre-Santos, *Asian J. Org. Chem.*, 2014, **3**, 185–197; (*m*) J. Ranta, K. Kaunisto, M. Niskanen, A. Efimov, T. I. Hukka and H. Lemmetyinen, *J. Phys. Chem. C*, 2014, **118**, 2754–2765.

4 O. Vostrowsky and A. Hirsch, *Chem. Rev.*, 2006, **106**, 5191–5207.

5 (*a*) J. C. Hummelen, B. Knight, J. Pavlovich, R. González and F. Wudl, *Science*, 1995, **269**, 1554–1556; (*b*) M. Keshavarz-K, R. Gonzalez, R. G. Hicks, G. Srdanov, V. I. Srdanov, T. G. Collins, J. C. Hummelen, C. Bellavia-Lund, J. Pavlovich, F. Wudl and K. Holczer, *Nature*, 1996, **383**, 147–150; (*c*) M. Keshavarz-K, R. Gonzalez, R. G. Hicks, G. Srdanov, V. I. Srdanov, T. G. Collins, J. C. Hummelen, C. Bellavia-Lund, J. Pavlovich, F. Wudl and K. Holczer, *Nature*, 1996, **383**, 147–150; (*d*) C. Bellavia-Lund, R. González, J. C. Hummelen, R. G. Hicks, A. Sastre and F. Wudl, *J. Am. Chem. Soc.*, 1997, **119**, 2946–2947.

6 F. Hauke and A. Hirsch, *Chem. Commun.*, 1999, 2199–2200.

7 (*a*) F. Hauke, A. Swartz, D. M. Guldi and A. Hirsch, *J. Mater. Chem.*, 2002, **12**, 2088–2094; (*b*) F. Hauke, S. Atalick, D. M. Guldi and A. Hirsch, *Tetrahedron*, 2006, **62**, 1923–1927.

8 F. Hauke, A. Hirsch, S. Atalick and D. M. Guldi, *Eur. J. Org. Chem.*, 2005, 1741–1751.

9 G. Rotas, J. Ranta, A. Efimov, M. Niemi, H. Lemmetyinen, N. Tkachenko and N. Tagmatarchis, *ChemPhysChem*, 2012, **13**, 1246–1254.

10 G. Rotas, G. Charalambidis, L. Glätzl, D. T. Gryko, A. Kahnt, A. G. Coutsolelos and N. Tagmatarchis, *Chem. Commun.*, 2013, **49**, 9128–9130.

11 (*a*) C. Huang, S. Barlow and S. R. Marder, *J. Org. Chem.*, 2011, **76**, 2386–2407; (*b*) C. Li and H. Wonneberger, *Adv. Mater.*, 2012, **24**, 613–636; (*c*) E. Kozma and M. Catellani, *Dyes Pigm.*, 2013, **98**, 160–179; (*d*) M. Guide, S. Pla, A. Sharenko, P. Zalar, F. Fernández-Lázaro, Á. Sastre-Santos and T.-Q. Nguyen, *Phys. Chem. Chem. Phys.*, 2013, **15**, 18894–18899; (*e*) Q. Yan, Y. Zhou, Y.-Q. Zheng, J. Pei and D. Zhao, *Chem. Sci.*, 2013, **4**, 4389–4394; (*f*) X. Zhang, Z. Lu, L. Ye, C. Zhan, J. Hou, S. Zhang, B. Jiang, Y. Zhao,

J. Huang, S. Zhang, Y. Liu, Q. Shi, Y. Liu and J. Yao, *Adv. Mater.*, 2013, **25**, 5791–5797; (*g*) R. Shivanna, S. Shoaee, S. Dimitrov, S. K. Kandappa, S. Rajaram, J. R. Durrant and K. S. Narayan, *Energy Environ. Sci.*, 2014, **7**, 435–441.

12 (*a*) Y. Shibano, T. Umeyama, Y. Matano, N. V. Tkachenko, H. Lemmetyinen and H. Imahori, *Org. Lett.*, 2006, **8**, 4425–4428; (*b*) R. K. Dubey, M. Niemi, K. Kaunisto, A. Efimov, N. V. Tkachenko and H. Lemmetyinen, *Chem. – Eur. J.*, 2013, **19**, 6791–6806.

13 Y. Liu and J. Zhao, *Chem. Commun.*, 2012, **48**, 3751–3753.

14 H. Ito, T. Tada, M. Sudo, Y. Ishida, T. Hino and K. Saigo, *Org. Lett.*, 2003, **5**, 2643–2645.

15 E. M. Pérez, M. Sierra, L. Sánchez, M. R. Torres, R. Viruela, P. M. Viruela, E. Ortí and N. Martín, *Angew. Chem., Int. Ed.*, 2007, **46**, 1847–1851.

16 (*a*) S. Prathapan, S. I. Yang, J. Seth, M. A. Miller, D. F. Bocian, D. Holten and J. S. Lindsey, *J. Phys. Chem. B*, 2001, **105**, 8237–8248; (*b*) W. E. Ford and P. V. Kamat, *J. Phys. Chem.*, 1987, **91**, 6373–6380.

17 Y. Shibano, T. Umeyama, Y. Matano, N. V. Tkachenko, H. Lemmetyinen and H. Imahori, *Org. Lett.*, 2006, **8**, 4425–4428.

18 R. A. Marcus, *Angew. Chem., Int. Ed. Engl.*, 1993, **32**, 1111–1121.